Hybrid modeling of redshift space distortions

Yi ZHENG (郑逸)
Korea Institute of Advanced Study (KIAS)

Yong-Seon Song, Yi Zheng , Atsushi Taruya, and Minji Oh, 1801.04950

The 7th survey science group workshop, Jan. 15-17 2018, High-1

RSD Introduction

Redshift space distortion

In observation, galaxy distance is determined by “redshift”

Peculiar velocity of galaxies cause them to appear displaced along the line of sight in redshift space

For DESI

SDSS DR9. CMASS. 2D correlation

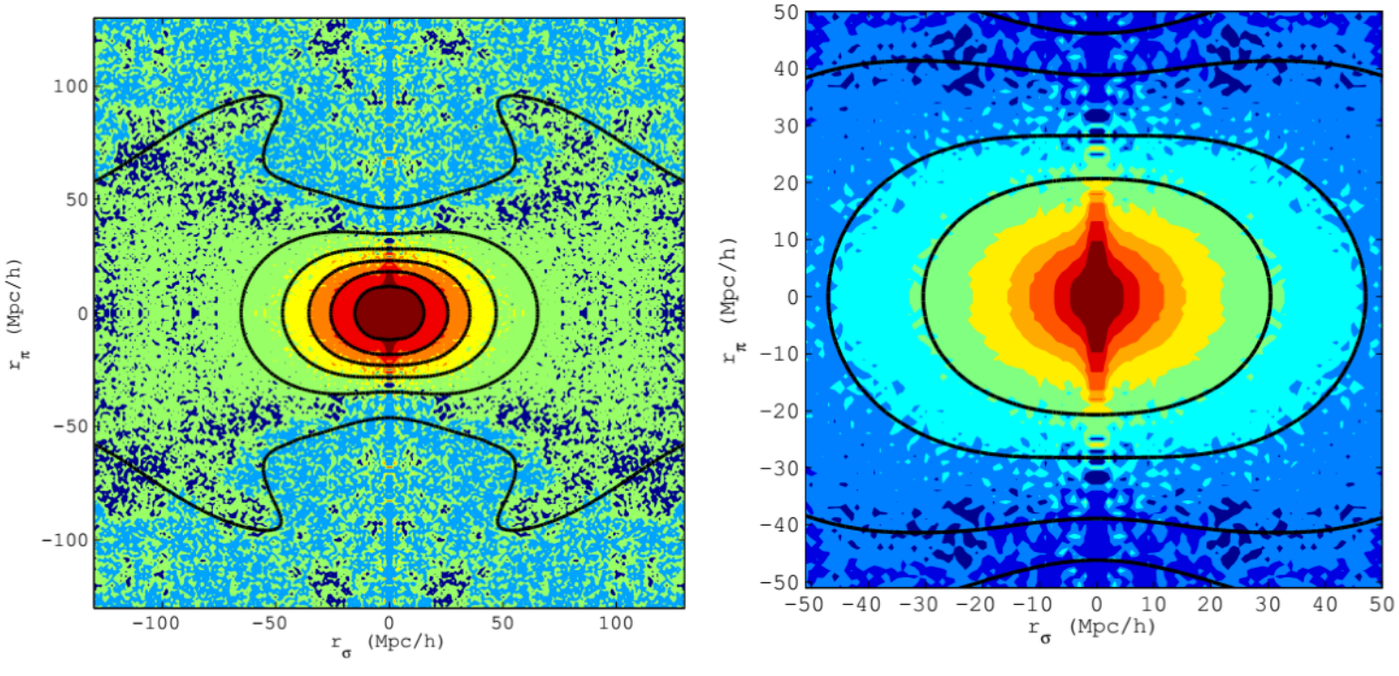

Figure 3. *Left panel*: Two-dimensional correlation function of CMASS galaxies (color) compared with the best fit model described in Section 6.1 (black lines). Contours of equal ξ are shown at [0.6, 0.2, 0.1, 0.05, 0.02, 0]. *Right panel*: Smaller-scale two-dimensional clustering. We show model contours at [0.14, 0.05, 0.01, 0]. The value of ξ_0 at the minimum separation bin in our analysis is shown as the innermost contour. The $\mu \approx 1$ “finger-of-god” effects are small on the scales we use in this analysis.

Reid et al. 1203.6641

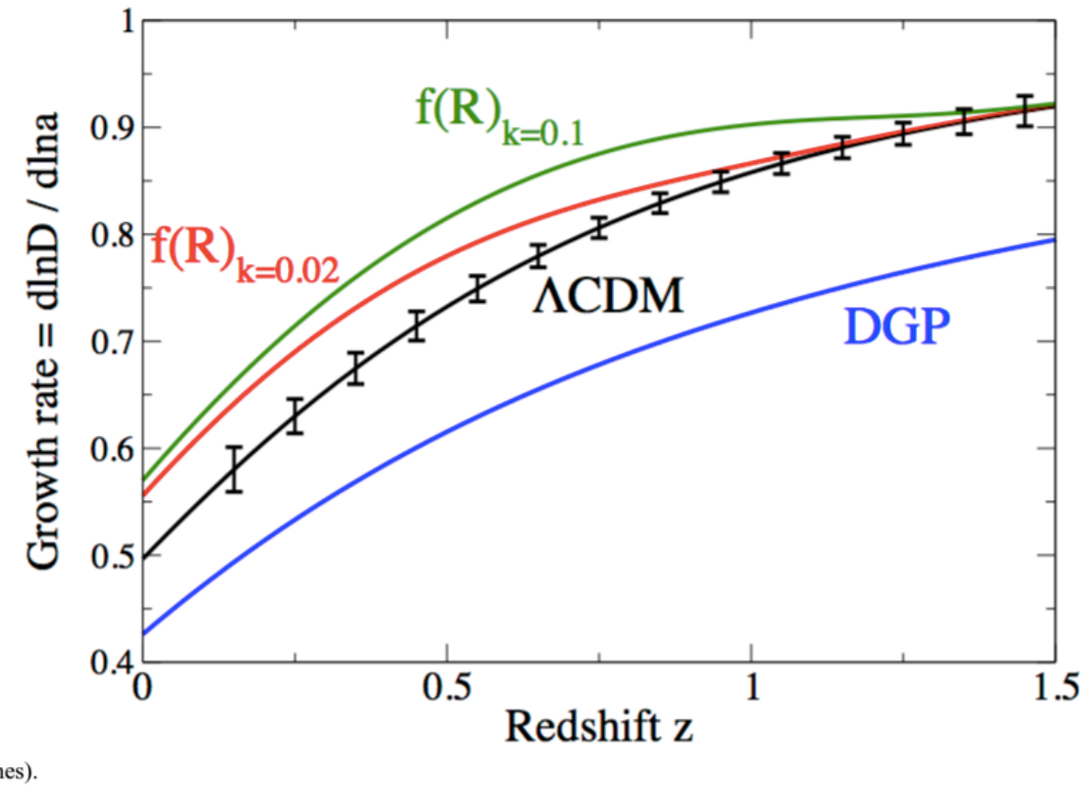

Huterer et al. 1309.5385

Redshift space distortion: small scale modelling and systematic errors

Observationally:

O(1%)

DESI, Euclid et all:

z	$\frac{\sigma_{f\sigma_{0.1}}}{f\sigma_{0.1}}$ %	$\frac{\sigma_{f\sigma_{0.2}}}{f\sigma_{0.2}}$ %
0.65	3.31	1.57
0.75	2.10	1.01
0.85	2.12	1.01
0.95	2.09	0.99
1.05	2.23	1.11
1.15	2.25	1.14
1.25	2.25	1.16
1.35	2.90	1.73
1.45	3.06	1.87
1.55	3.53	2.27
1.65	5.10	3.61
1.75	8.91	6.81
1.85	9.25	7.07

DESI forcast

1611.00036

$$N_k \propto k^3$$

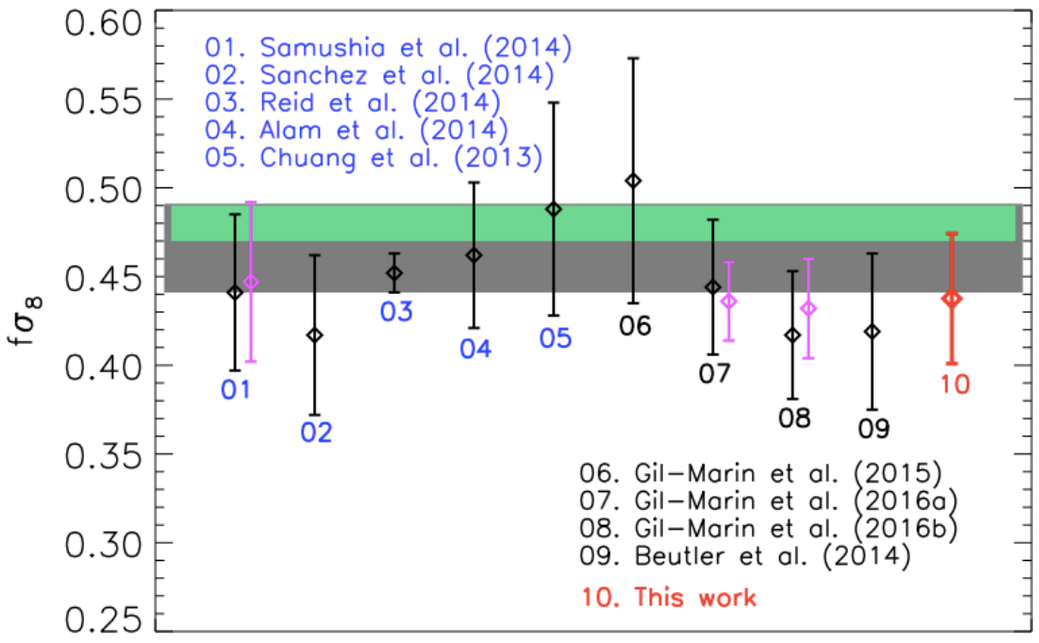

Figure 8. Constraints on $f(z_{\rm eff})\sigma_8(z_{\rm eff})$ from BOSS CMASS DR10, DR11, and DR12 releases. Our result are shown as a red diamond. Black diamonds

1609.03697

Redshift space distortion modelling II: in general three steps

1. Non-linear mapping of dark matter/halo/galaxy clustering from real space to redshift space

$$P^{(\mathrm{S})}(k,\mu) = \int d^3\boldsymbol{x}\, e^{i\,\boldsymbol{k}\cdot\boldsymbol{x}} \left\langle e^{j_1 A_1} A_2 A_3 \right\rangle$$

2.Non-linear evolution of density and velocity fields

——— Perturbation theory & High-resolution simulations

$$\delta_n(\mathbf{k}) = \int \mathrm{d}^3\mathbf{q}_1 \cdots \int \mathrm{d}^3\mathbf{q}_n\, \delta_{\mathrm{D}}(\mathbf{k} - \mathbf{q}_{1\cdots n}) F_n(\mathbf{q}_1,\ldots,\mathbf{q}_n)\delta_1(\mathbf{q}_1)\cdots\delta_1(\mathbf{q}_n)\,,$$

$$\theta_n(\mathbf{k}) = \int \mathrm{d}^3\mathbf{q}_1 \cdots \int \mathrm{d}^3\mathbf{q}_n\, \delta_{\mathrm{D}}(\mathbf{k} - \mathbf{q}_{1\cdots n}) G_n(\mathbf{q}_1,\ldots,\mathbf{q}_n)\delta_1(\mathbf{q}_1)\cdots\delta_1(\mathbf{q}_n)\,,$$

F. Bernardeau et al, 2002

3. Galaxy/halo density and velocity bias modelling

$$\delta_g(\boldsymbol{x}) = b_1\delta(\boldsymbol{x}) + \frac{1}{2}b_2[\delta(\boldsymbol{x})^2 - \sigma_2] + \frac{1}{2}b_{s^2}[s(\boldsymbol{x})^2 - \langle s^2\rangle] + \text{higher order terms},$$

McDonald&Roy, 0902.0991

1. Non-linear mapping of dark matter/halo/galaxy clustering from real space to redshift space

Extended TNS model strategy, 1603.00101

$$P^{(\mathrm{S})}(k,\mu) = D^{\mathrm{FoG}}(k\mu\sigma_z)P_{\mathrm{perturbed}}(k,\mu)$$
$$= D^{\mathrm{FoG}}(k\mu\sigma_z)[P_{\delta\delta} + 2\mu^2 P_{\delta\Theta} + \mu^4 P_{\Theta\Theta}$$
$$+ A(k,\mu) + B(k,\mu) + T(k,\mu) + F(k,\mu)].$$

$$D^{\mathrm{FoG}}(k\mu\sigma_z) = e^{-k^2\mu^2\sigma_z^2}$$

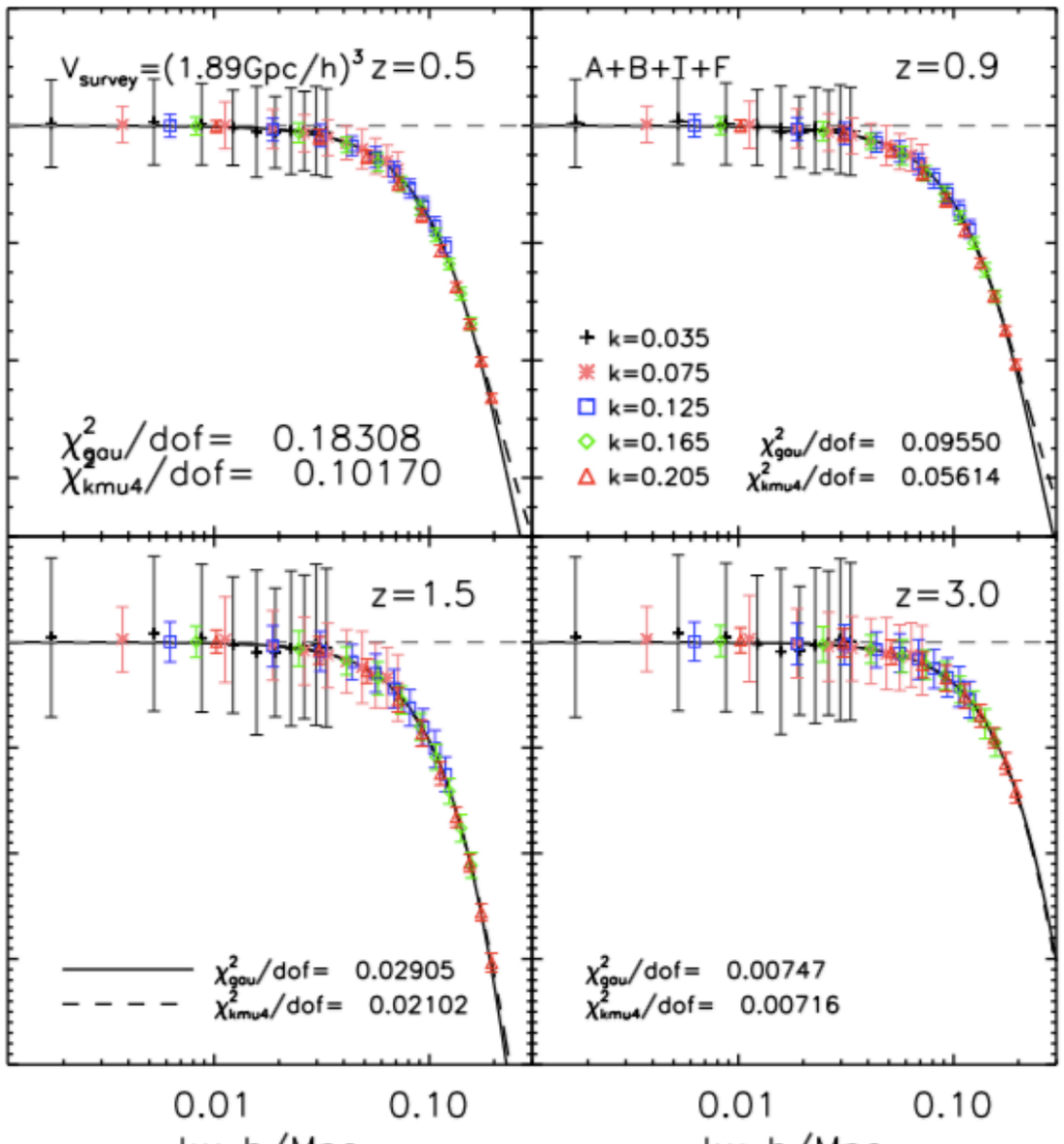

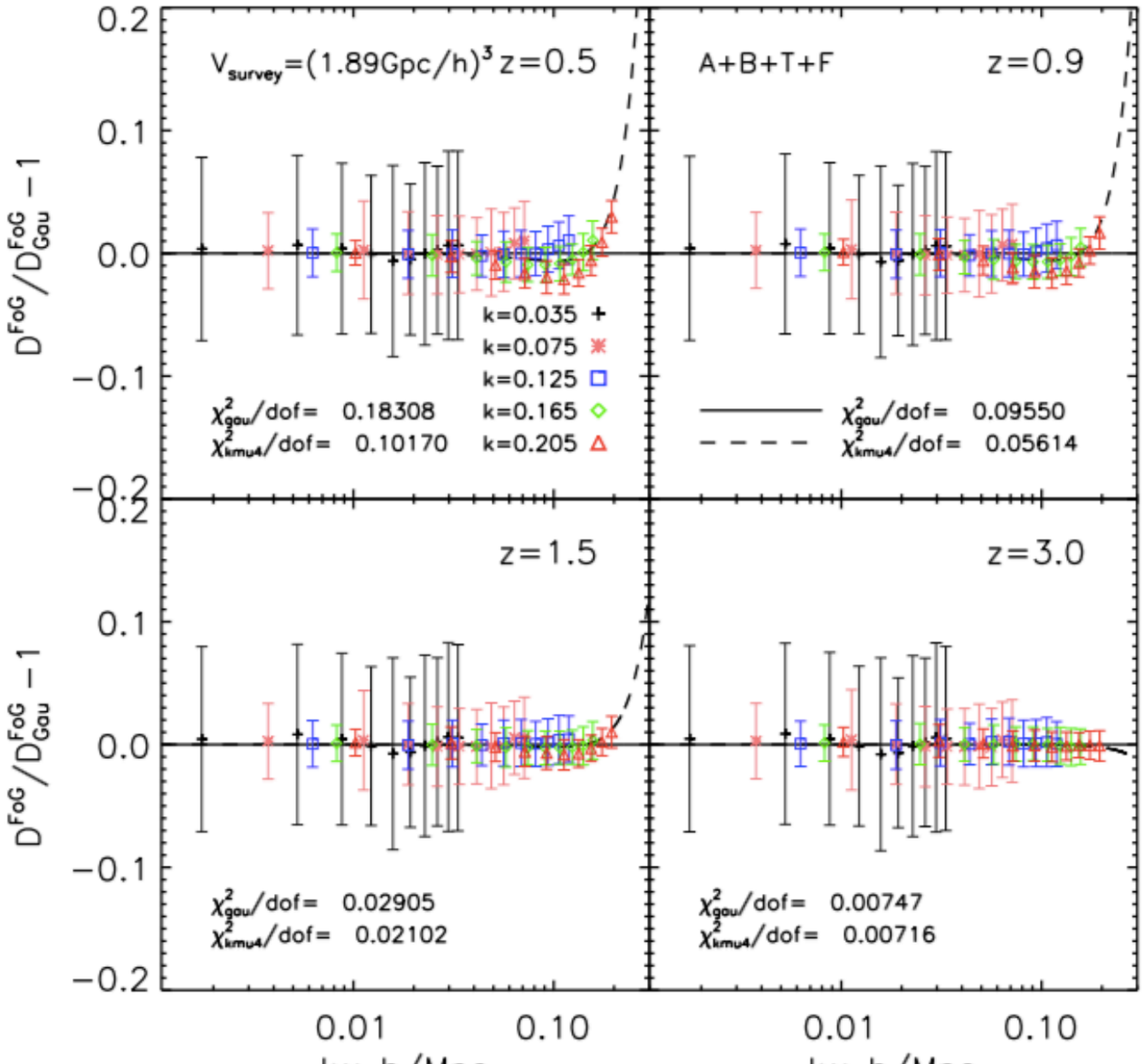

2.Non-linear evolution of density and velocity fields
——— Perturbation theory & High-resolution simulations

Starting from fiducial model: h=0.67, 100 realizations to varied cosmologies h=(0.57,0.62,0.72,0.77), 1 realization each with consistent broad band shape of power spectrum

All results are at z=0.5

2.1 Hybrid modeling of P_xy

$$\bar{P}_{XY}(k,z) = \bar{P}^{\rm th}_{XY}(k,z) + \bar{P}^{\rm res}_{XY}(k,z),$$

$$P^{\rm res}_{XY} = \left(\frac{G_X\, G_Y\, G_\delta^4}{\bar{G}_X \bar{G}_Y\, \bar{G}_\delta^4}\right) \bar{P}^{\rm res}_{XY},$$

$$P_{XY}(k) = P^{\rm th}_{XY}(k,z) + P^{\rm res}_{XY}(k,z)$$

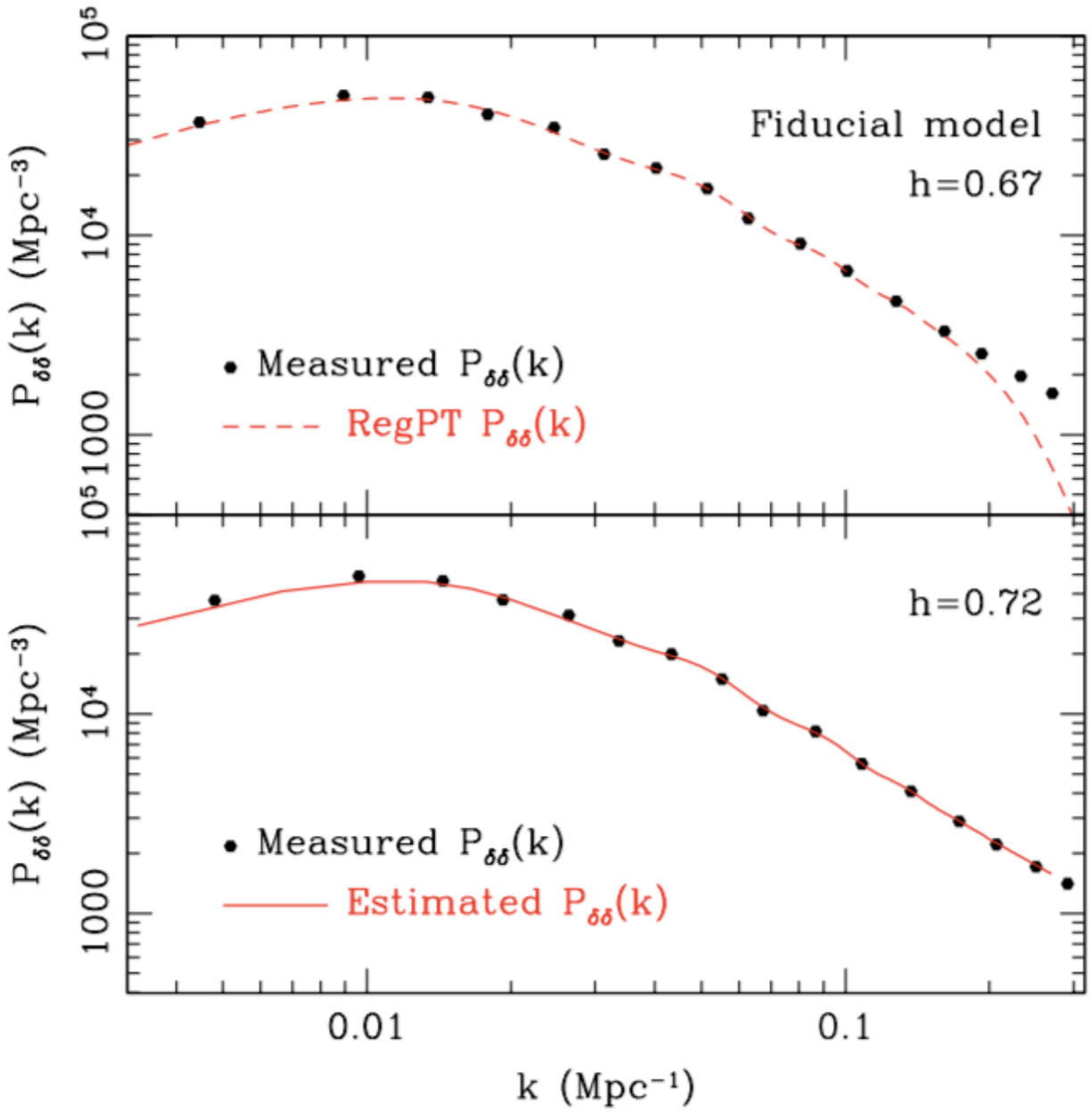

2.1 Hybrid modeling of P_xy

x,y: density or velocity

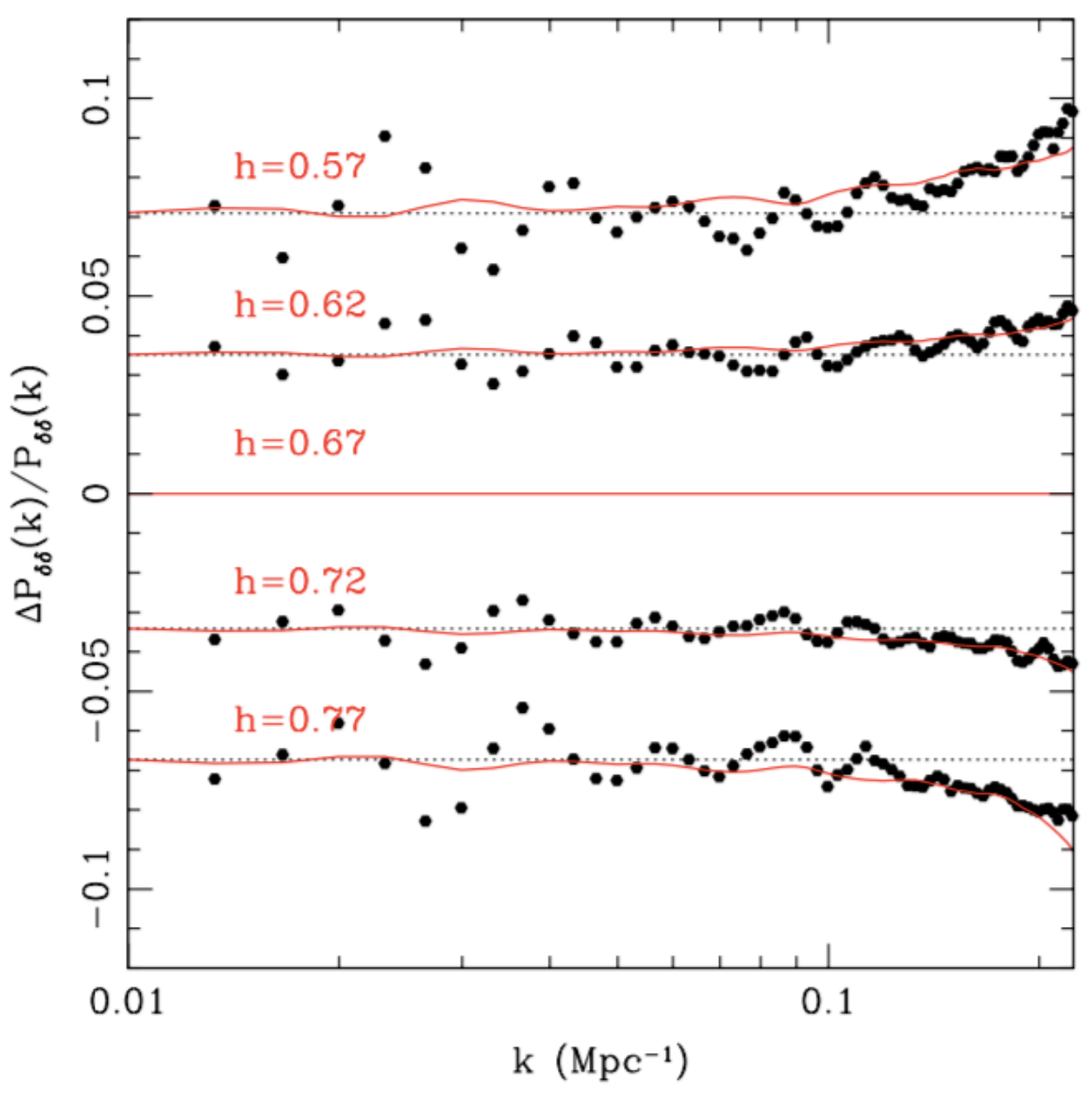

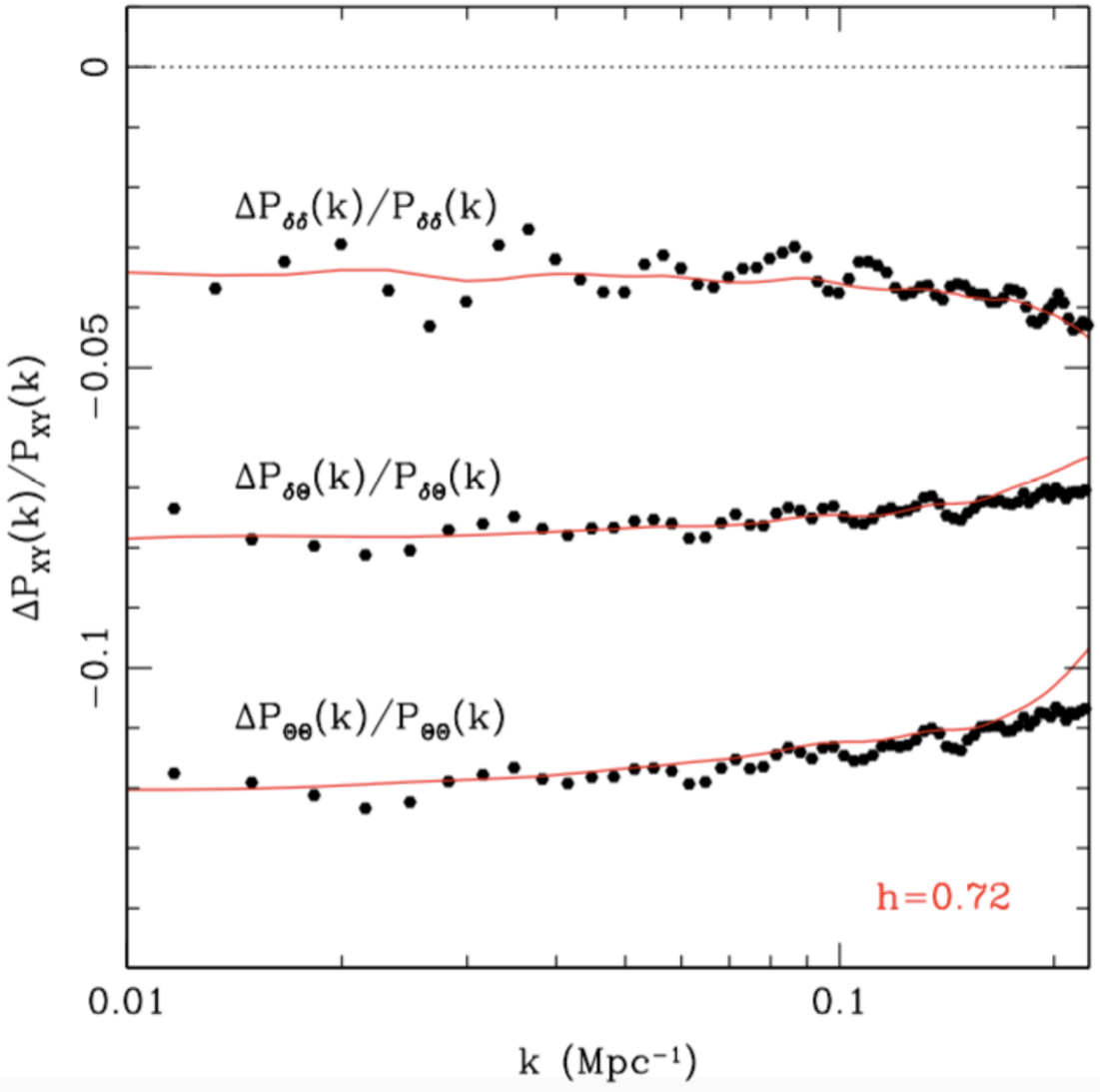

treatment is further tested for $P_{\delta\Theta}$ and $P_{\Theta\Theta}$ in the fiducial model. The predicted power spectra are pretty much consistent with measured results of power spectrum difference at $k \lesssim 0.2\,\mathrm{Mpc}^{-1}$.

2.2 Hybrid modeling of higher order corrections

$$P^{(S)}(k,\mu) = D^{FoG}(k\mu\sigma_z)P_{perturbed}(k,\mu)$$
$$= D^{FoG}(k\mu\sigma_z)[P_{\delta\delta} + 2\mu^2 P_{\delta\Theta} + \mu^4 P_{\Theta\Theta}$$
$$+ A(k,\mu) + B(k,\mu) + T(k,\mu) + F(k,\mu)].$$

Assumption: the time-dependence of each term is approximately determined by the leading-order growth factor dependence of u_z and δ

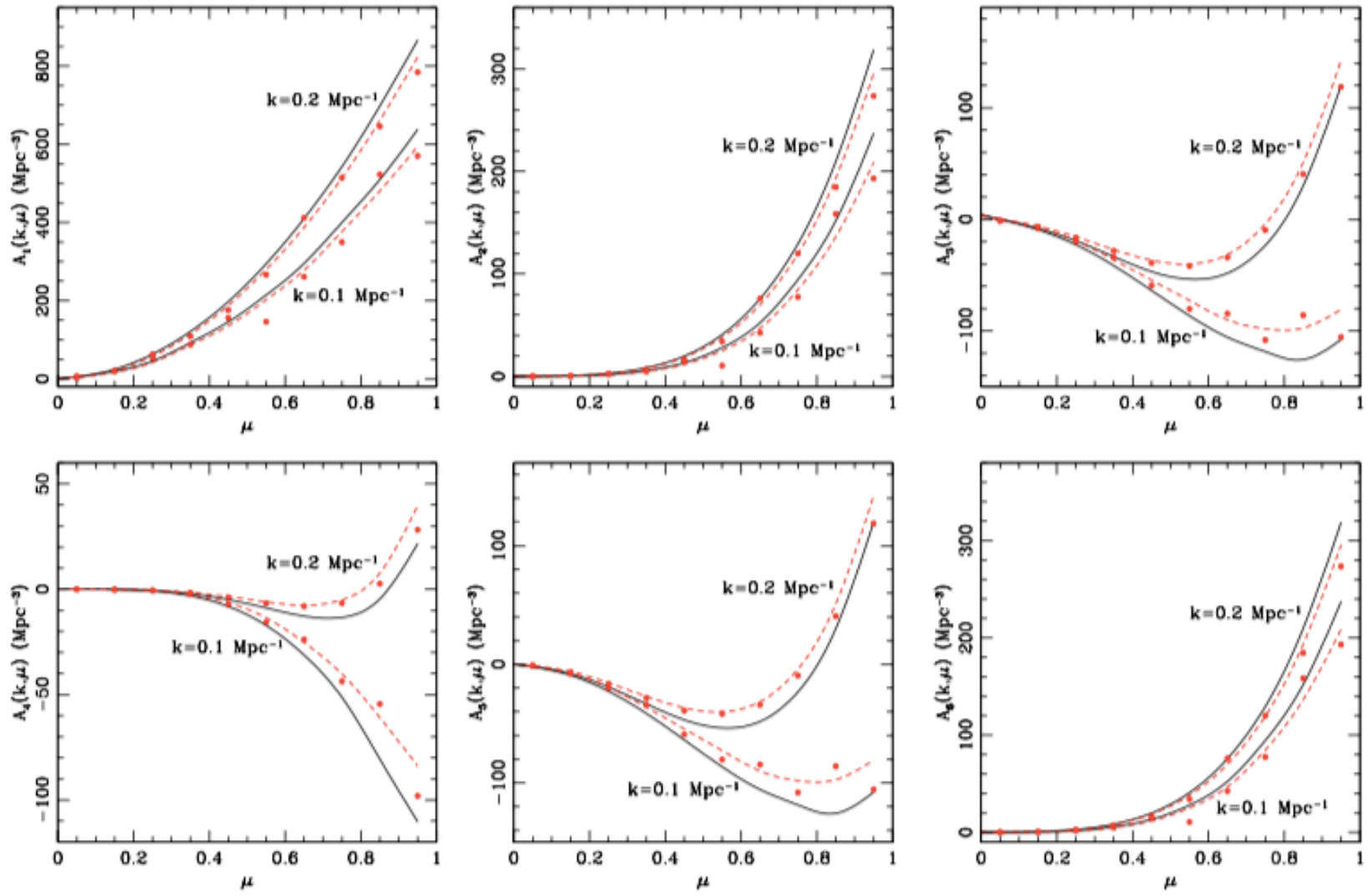

A term

$$\bar{A}(k,\mu) = j_1 \int d^3\boldsymbol{x}\; e^{i\boldsymbol{k}\cdot\boldsymbol{x}}\; \langle A_1 A_2 A_3 \rangle_c$$
$$= \sum_{n=1}^{6} \bar{\mathcal{A}}_n$$

$$A(k,\mu) = \sum_{n=1}^{6} \mathcal{A}_n$$
$$= (G_\delta/\bar{G}_\delta)^2 (G_\Theta/\bar{G}_\Theta)\,\bar{\mathcal{A}}_1 + (G_\delta/\bar{G}_\delta)(G_\Theta/\bar{G}_\Theta)^2\,\bar{\mathcal{A}}_2$$
$$+ (G_\delta/\bar{G}_\delta)(G_\Theta/\bar{G}_\Theta)^2\,\bar{\mathcal{A}}_3 + (G_\Theta/\bar{G}_\Theta)^3\,\bar{\mathcal{A}}_4$$
$$+ (G_\delta/\bar{G}_\delta)(G_\Theta/\bar{G}_\Theta)^2\,\bar{\mathcal{A}}_5 + (G_\delta/\bar{G}_\delta)(G_\Theta/\bar{G}_\Theta)^2\,\bar{\mathcal{A}}_6$$

Key results from now on:
Cosmological fitting combining step 1 and step 2

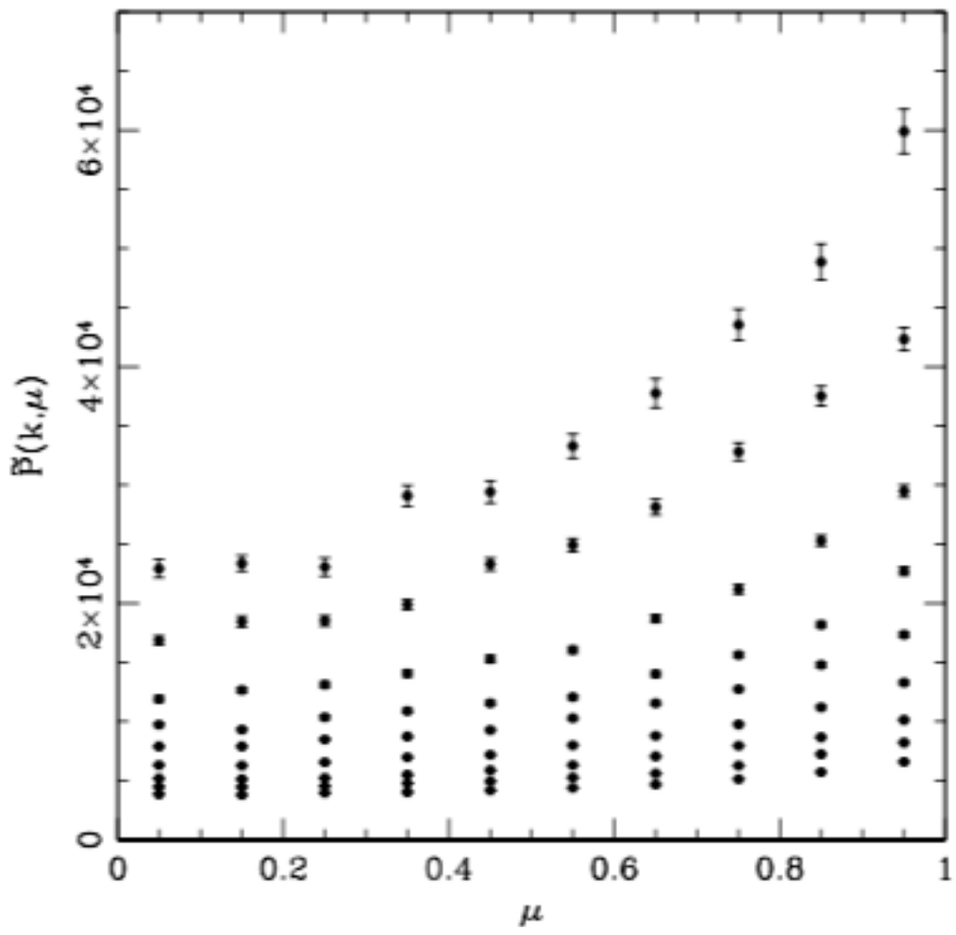

$$\mathrm{Cov}_{pp}^{-1}(k_i) = \frac{1}{\sigma[\tilde{P}_{\mathrm{ob}}(k_i,\mu_p)]^2}\,.$$

Figure 7. Redshift-space power spectrum at $z = 0.5$, measured from N-body simulations. The mean values of the power spectrum, $\tilde{P}_{\mathrm{ob}}(k,\mu)$, are estimated using 100 realizations of the simulation data, and results are plotted as function of directional cosine μ at the wavenumbers $k = 0.055$, 0.075, 0.095, 0.115, 0.135, 0.155, 0.175, 0.195, and $0.215\,h\,\mathrm{Mpc}^{-1}$ (from top to bottom), together with their 1σ error.

$$\chi^2 = \sum_{i=i_{\mathrm{min}}}^{i_{\mathrm{max}}} \sum_{p=1}^{10}\sum_{q=1}^{10} [\tilde{P}_{\mathrm{obs}}(k_i,\mu_p) - \tilde{P}_{\mathrm{model}}(k_i,\mu_p)]\mathrm{Cov}_{pq}^{-1}(k_i)[\tilde{P}_{\mathrm{obs}}(k_i,\mu_q) - \tilde{P}_{\mathrm{model}}(k_i,\mu_q)]$$

Chi^2 results: fiducial model

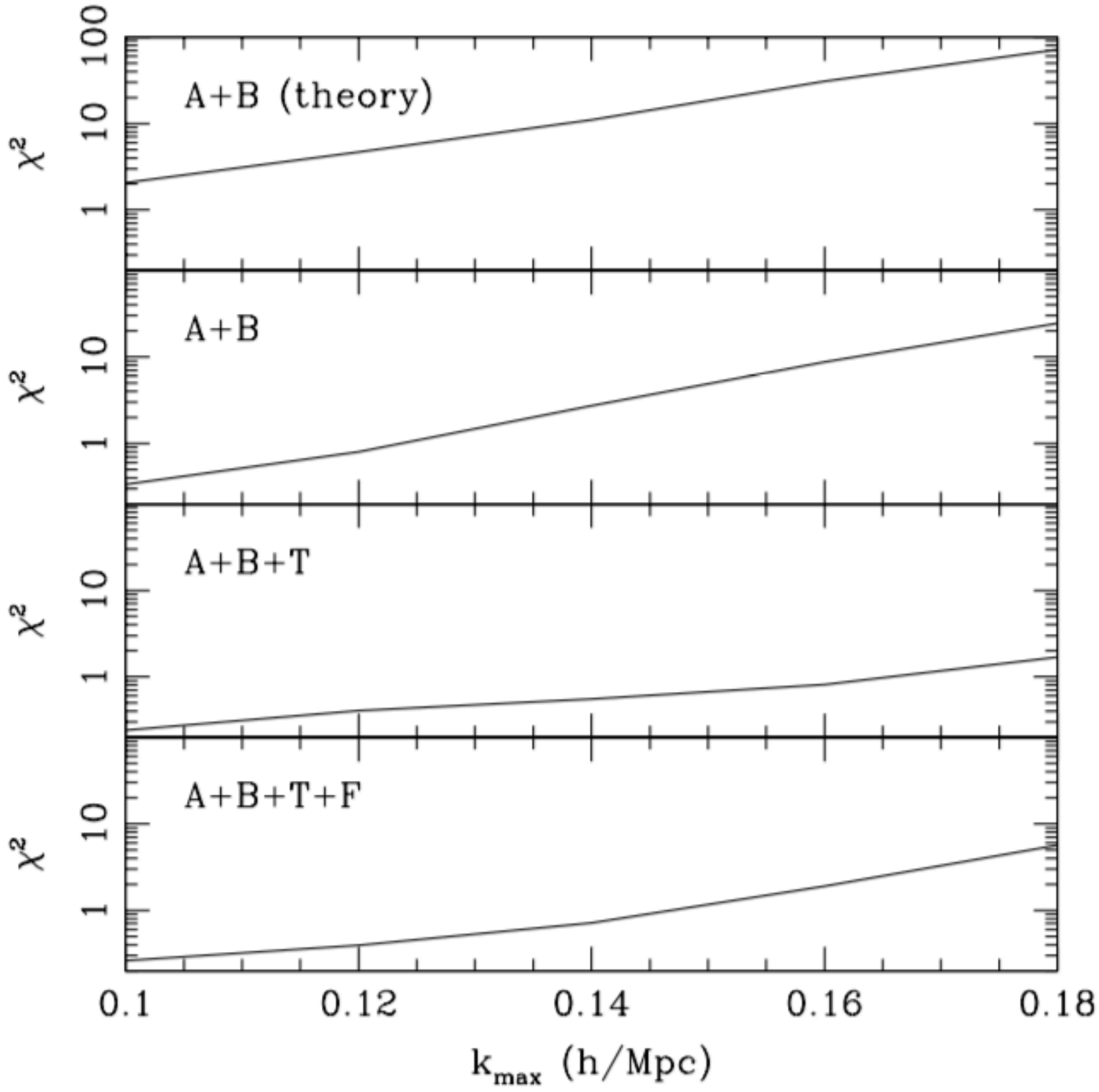

We try combinations of higher order terms:
A+B(theory), A+B, A+B+T, A+B+T+F

Linear density growth factor and growth rate reconstruction: fiducial model

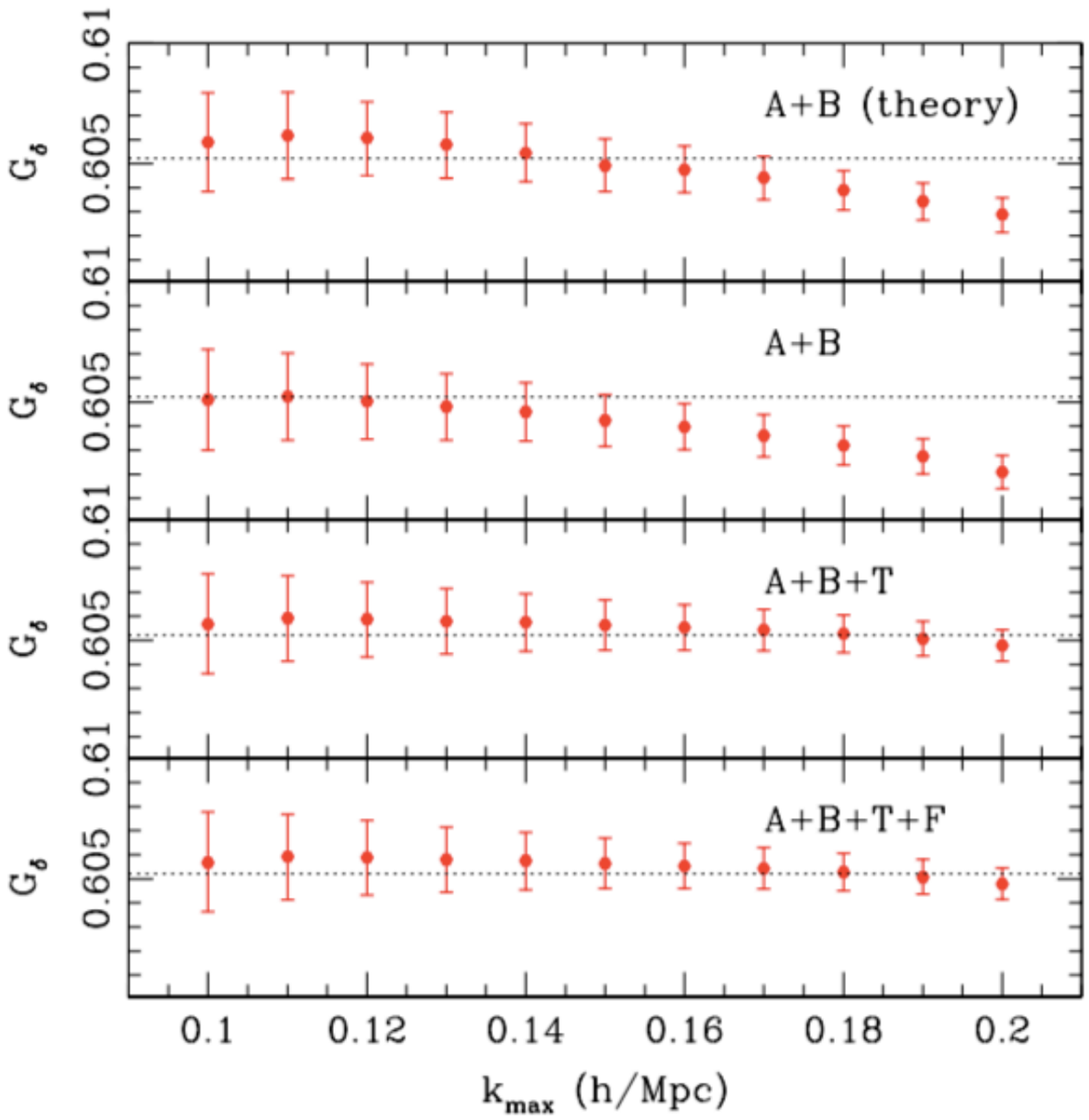

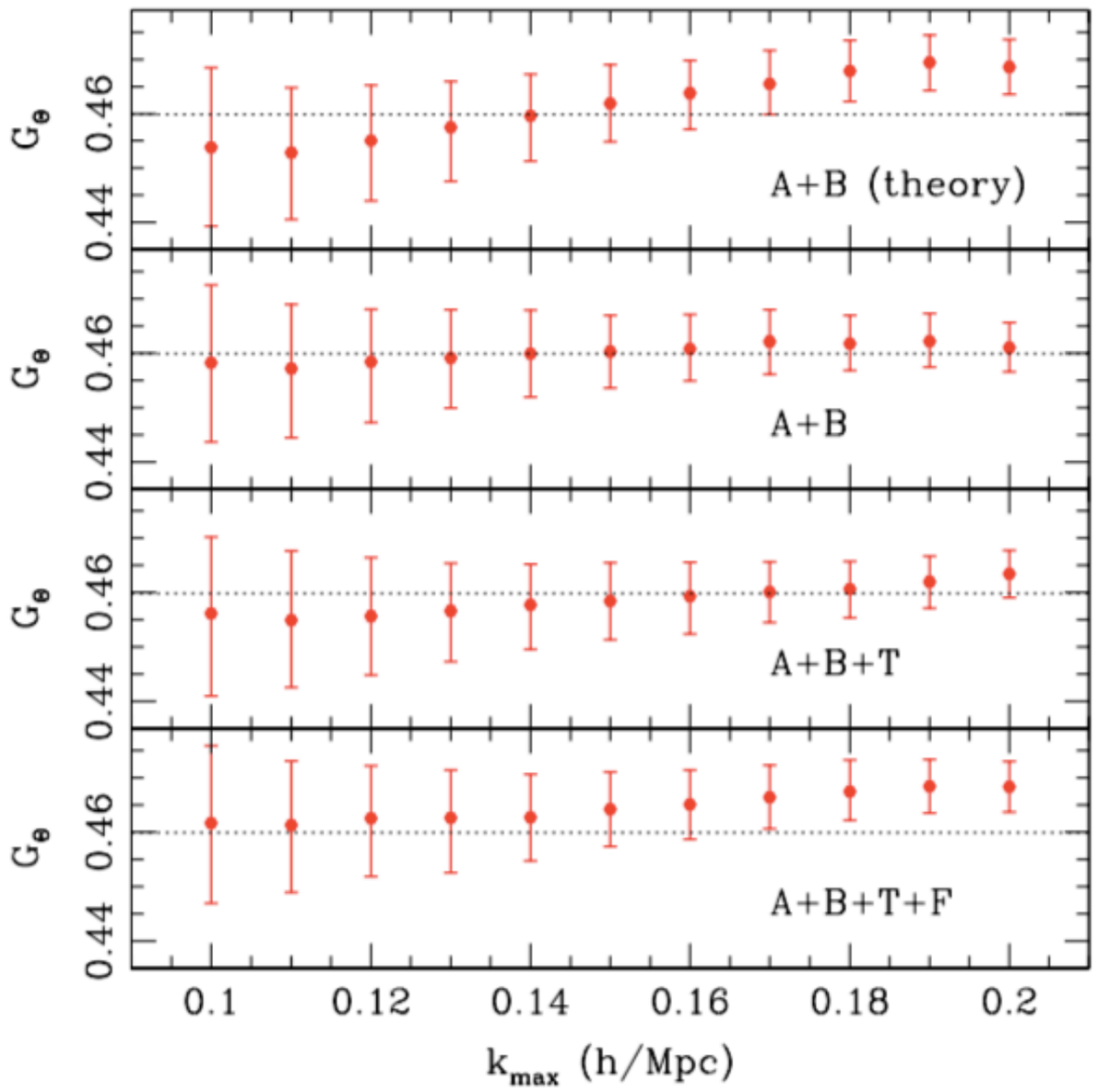

Linear density growth factor and growth rate reconstruction: varied cosmological models

$$k \lesssim k_{\rm max} = 0.18\,h\,{\rm Mpc}^{-1}$$

A+B+T model

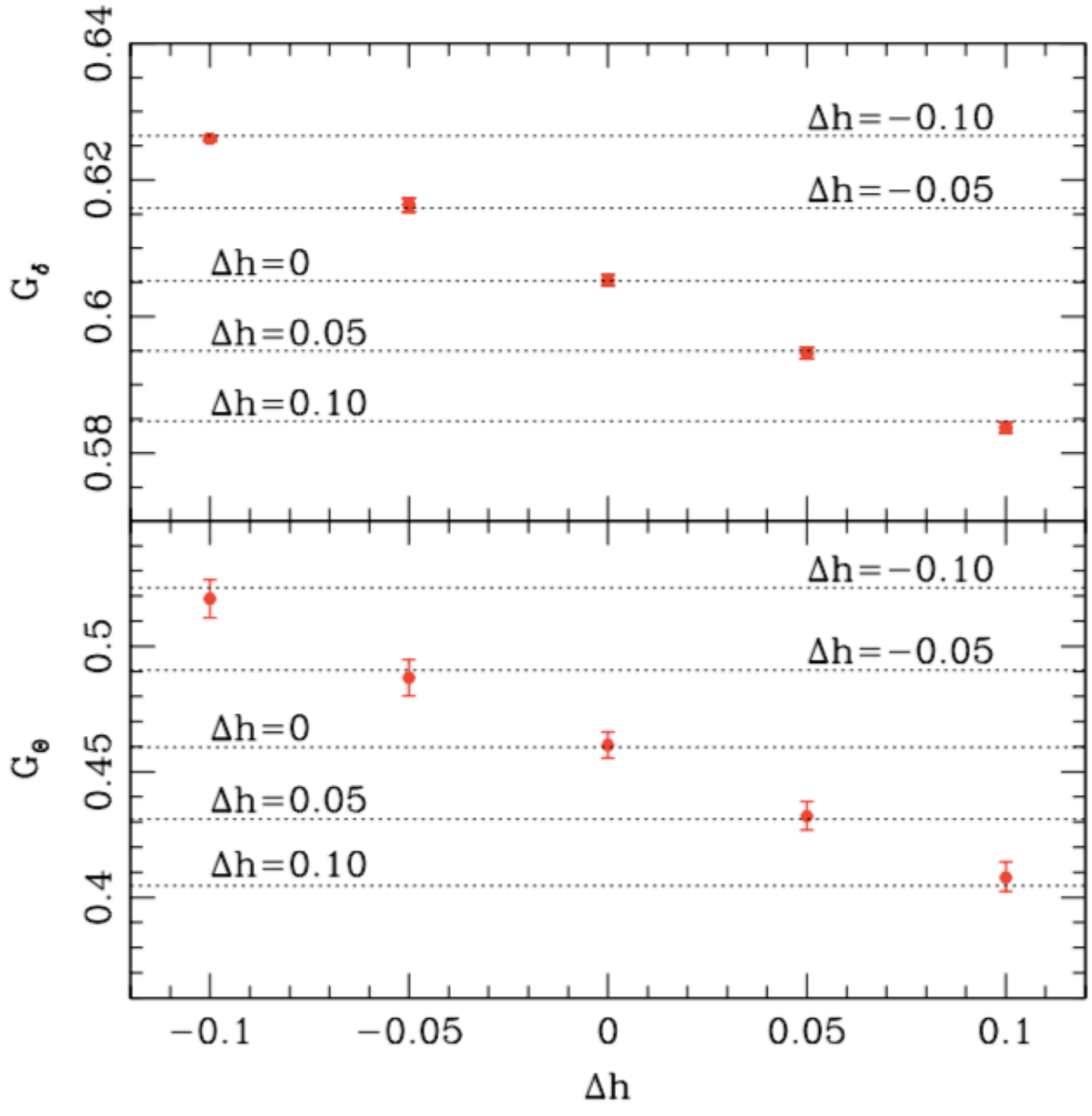

Discussions

- Step 3. galaxy/halo bias
  - halo —— dark matter: Yi Zheng et al. in preparation
  - galaxy —— halo: halo model, e.g. 1706.02362

- To seek a flexible template in which the broadband shape of the power spectrum is allowed to vary ——exploit the fast PT calculation as well as to find a more cleaver way to calibrate the power spectrum with N-body simulation.

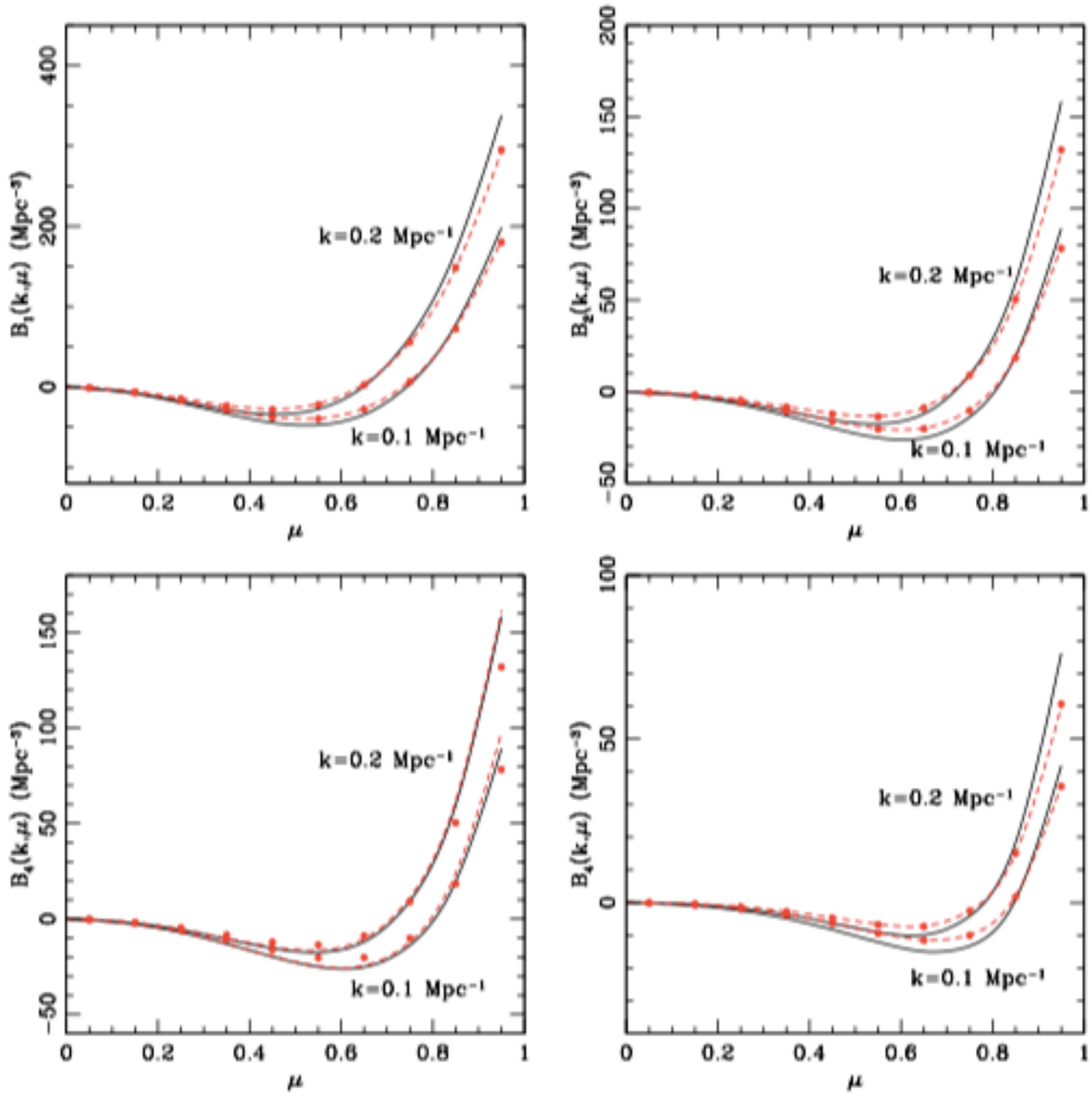

B term

$$\bar{B}(k,\mu) = j_1^2 \int d^3\boldsymbol{x}\; e^{i\boldsymbol{k}\cdot\boldsymbol{x}}\; \langle A_1 A_2\rangle_c \langle A_1 A_3\rangle_c$$

$$= \sum_{n=1}^{4} \bar{\mathcal{B}}_n$$

$$B(k,\mu) = \sum_{n=1}^{4} \mathcal{B}_n$$

$$= \left(G_\delta/\bar{G}_\delta\right)^2 \left(G_\Theta/\bar{G}_\Theta\right)^2 \bar{\mathcal{B}}_1 + \left(G_\delta/\bar{G}_\delta\right)\left(G_\Theta/\bar{G}_\Theta\right)^3 \bar{\mathcal{B}}_2$$

$$+ \left(G_\delta/\bar{G}_\delta\right)\left(G_\Theta/\bar{G}_\Theta\right)^3 \bar{\mathcal{B}}_3 + \left(G_\Theta/\bar{G}_\Theta\right)^4 \bar{\mathcal{B}}_4$$

3

F term

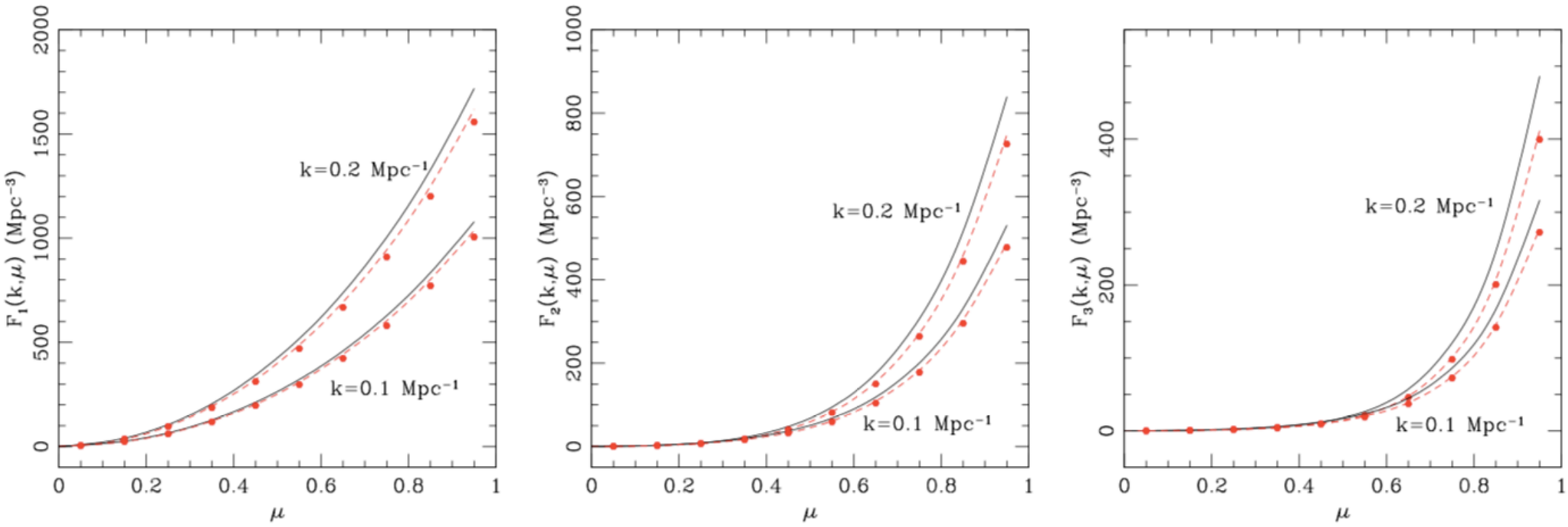

$$\bar{F}(k,\mu) = -j_1^2 \int d^3\boldsymbol{x}\; e^{i\boldsymbol{k}\cdot\boldsymbol{x}}\; \langle u_z u_z' \rangle_c \langle A_2 A_3 \rangle_c$$

$$= \sum_{n=1}^{3} \bar{\mathcal{F}}_n \;;$$

$$F(k,\mu) = \sum_{n=1}^{3} \mathcal{F}_n$$

$$= \left(G_\delta/\bar{G}_\delta\right)^2 \left(G_\Theta/\bar{G}_\Theta\right)^2 \bar{\mathcal{F}}_1 + \left(G_\delta/\bar{G}_\delta\right) \left(G_\Theta/\bar{G}_\Theta\right)^3 \bar{\mathcal{F}}_2 + \left(G_\Theta/\bar{G}_\Theta\right)^4 \bar{\mathcal{F}}_3$$

T term

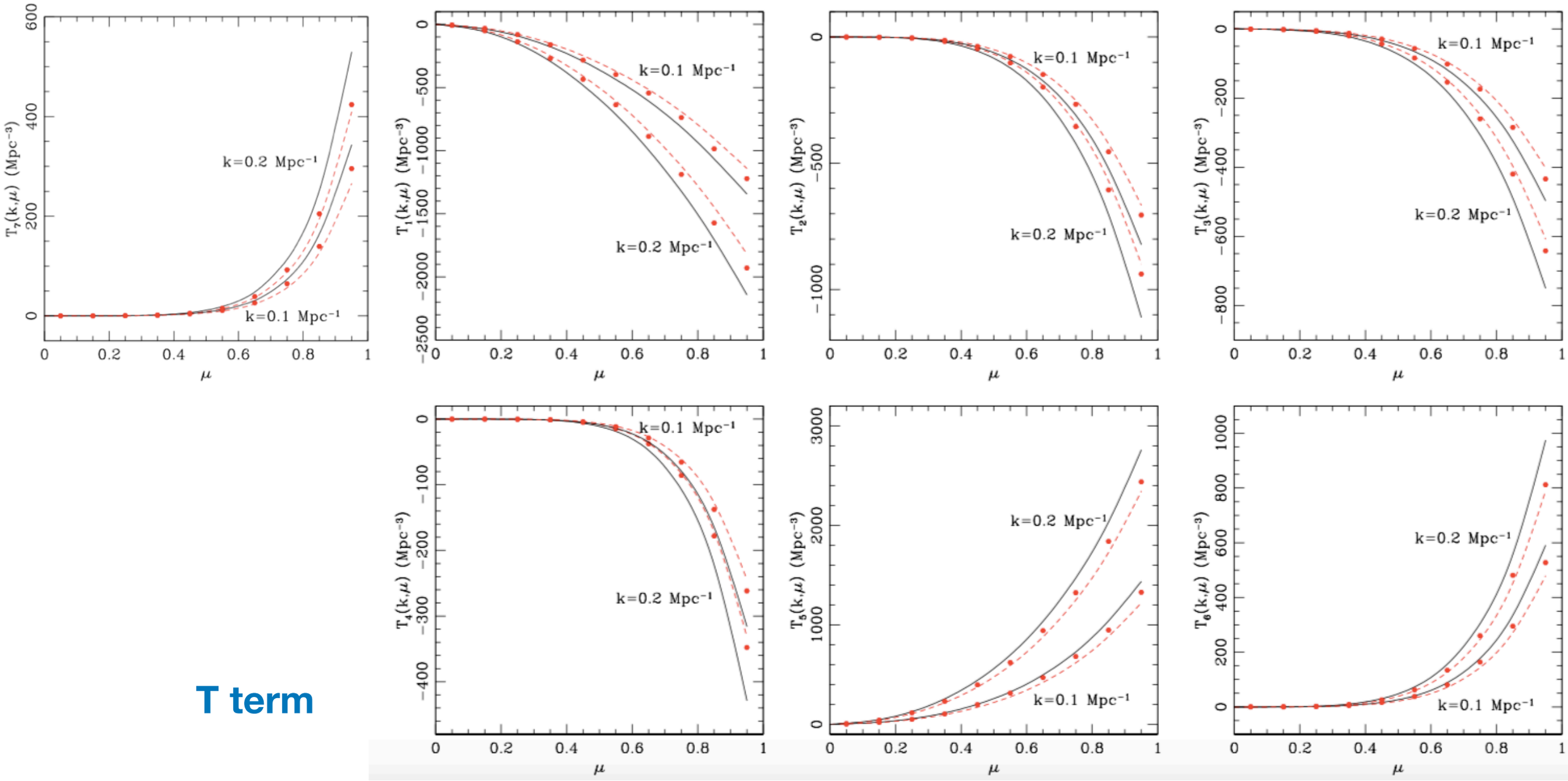

$$\bar{T}(k,\mu) = \frac{1}{2} j_1^2 \int d^3\boldsymbol{x}\; e^{i\boldsymbol{k}\cdot\boldsymbol{x}}\; \langle A_1^2 A_2 A_3 \rangle_c, \qquad T(k,\mu) = \sum_{n=1}^{7} \mathcal{T}_n \tag{2.39}$$

$$= \sum_{n=1}^{7} \bar{\mathcal{T}}_n\,;$$

$$= (G_\delta/\bar{G}_\delta)^2\,(G_\Theta/\bar{G}_\Theta)^2\,\bar{\mathcal{T}}_1 + (G_\delta/\bar{G}_\delta)\,(G_\Theta/\bar{G}_\Theta)^3\,\bar{\mathcal{T}}_2 + (G_\delta/\bar{G}_\delta)\,(G_\Theta/\bar{G}_\Theta)^3\,\bar{\mathcal{T}}_3$$

$$+ (G_\Theta/\bar{G}_\Theta)^4\,\bar{\mathcal{T}}_4 + (G_\delta/\bar{G}_\delta)^2\,(G_\Theta/\bar{G}_\Theta)^2\,\bar{\mathcal{T}}_5 + (G_\delta/\bar{G}_\delta)\,(G_\Theta/\bar{G}_\Theta)^3\,\bar{\mathcal{T}}_6 + (G_\Theta/\bar{G}_\Theta)^4\,\bar{\mathcal{T}}_7$$

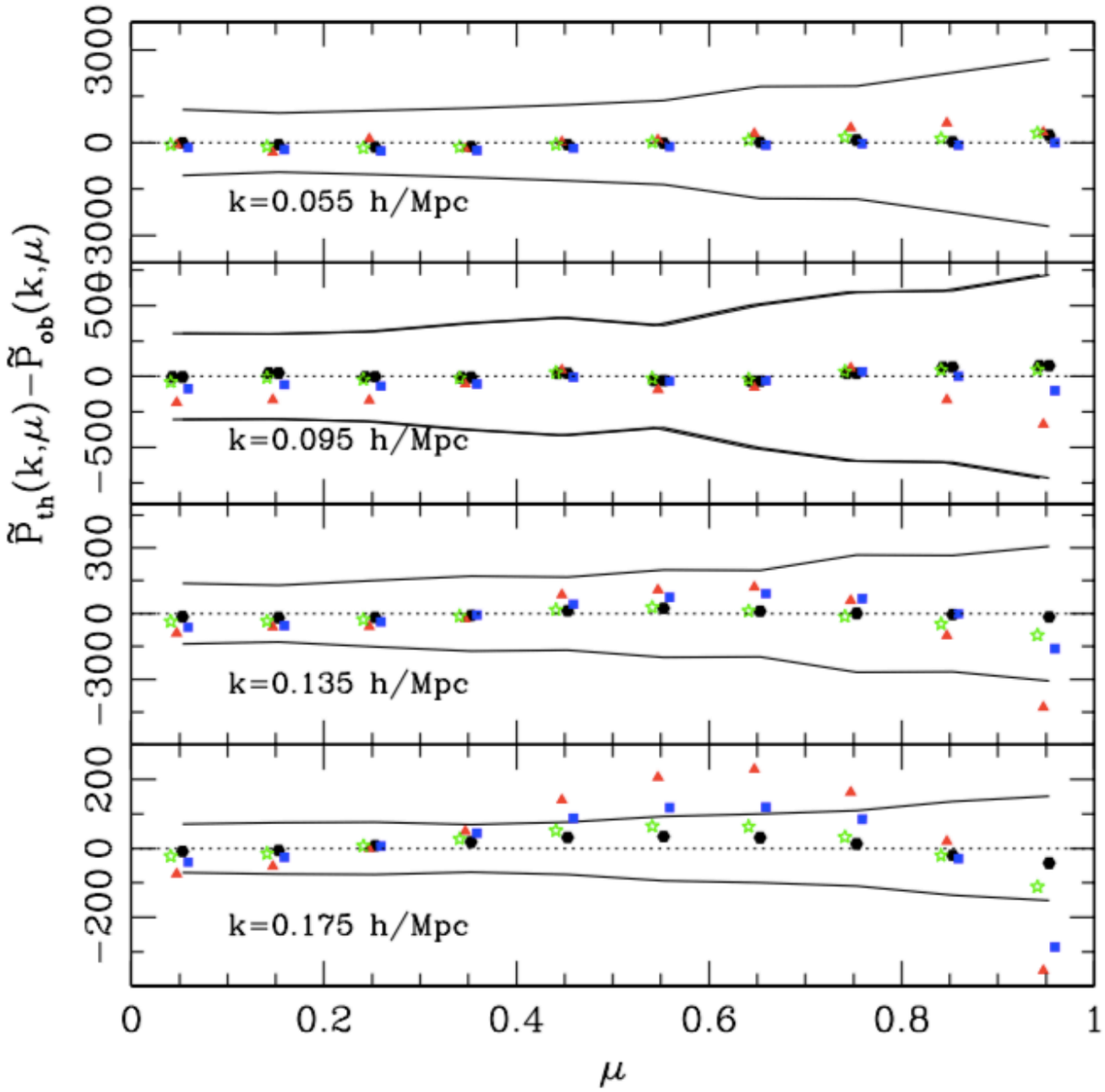
$\tilde{P}_{th}(k,\mu)-\tilde{P}_{ob}(k,\mu)$
k=0.055 h/Mpc
k=0.095 h/Mpc
k=0.135 h/Mpc
k=0.175 h/Mpc
μ

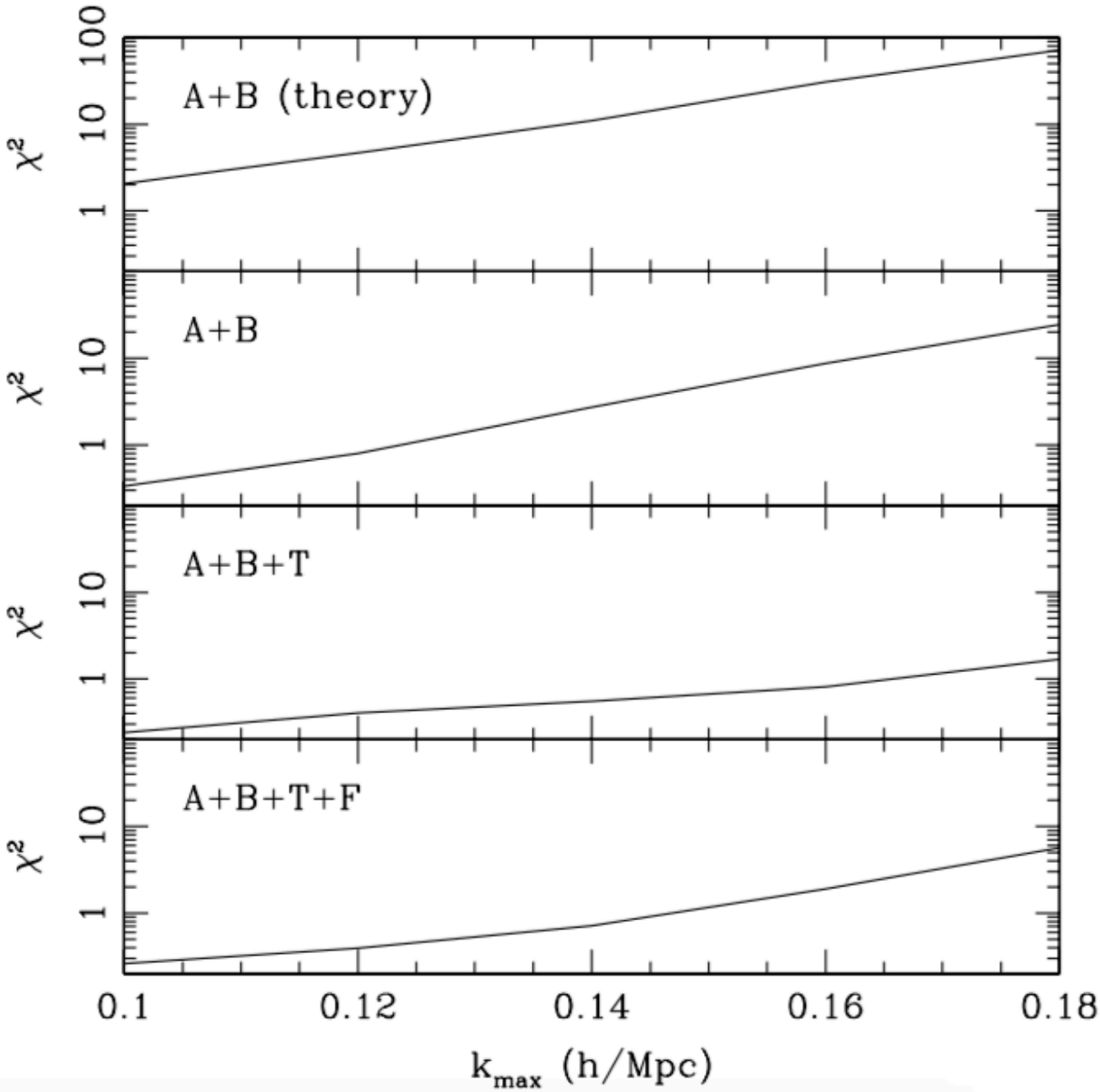
A+B (theory)
A+B
A+B+T
A+B+T+F
χ^2
k_{max} (h/Mpc)